# High-resolution imaging of bacterial spatial organization with vertical cell imaging by nanostructured immobilization (VerCINI)

Whitley, Kevin D.; Middlemiss, Stuart; Jukes, Calum; Dekker, Cees; Holden, Séamus

**DOI**
10.1038/s41596-021-00668-1

**Publication date**
2022

**Document Version**
Accepted author manuscript

**Published in**
Nature Protocols

**Citation (APA)**
Whitley, K. D., Middlemiss, S., Jukes, C., Dekker, C., & Holden, S. (2022). High-resolution imaging of bacterial spatial organization with vertical cell imaging by nanostructured immobilization (VerCINI). *Nature Protocols*, *17*(3), 847-869. https://doi.org/10.1038/s41596-021-00668-1

# High-resolution imaging of bacterial spatial organisation with Vertical Cell Imaging by Nanostructured Immobilisation (VerCINI)

Kevin D. Whitley[1,2*], Stuart Middlemiss[1], Calum Jukes[1], Cees Dekker[2], Séamus Holden[1*]

[1]Centre for Bacterial Cell Biology, Newcastle University, UK; [2]Department of Bionanoscience, Kavli Institute of Nanoscience Delft, Delft University of Technology, The Netherlands

*Corresponding authors: kevin.whitley@ncl.ac.uk, seamus.holden@ncl.ac.uk

## ABSTRACT

Light microscopy is indispensable for analysis of bacterial spatial organisation, yet the size and shapes of bacterial cells pose unique challenges to imaging. Bacterial cells are not much larger than the diffraction limit of visible light, and many species have cylindrical shapes and so lie flat on microscope coverslips, yielding low-resolution images when observing their short axes. In this protocol, we describe a pair of recently developed methods named VerCINI (Vertical Cell Imaging by Nanostructured Immobilisation) and µVerCINI (Microfluidic VerCINI) that greatly increase spatial resolution and image quality for microscopy of the short axes of bacteria. The concept behind both methods is that cells are imaged while confined vertically inside cell traps made from a nanofabricated mould. The mould is a patterned silicon wafer produced in a cleanroom facility using electron-beam lithography and deep reactive ion etching, which takes ~3 hrs for fabrication and ~12 hrs for surface passivation. After obtaining a mould, the entire process of making cell traps, imaging cells, and processing images can take ~2-12 hrs, depending on the experiment being done. VerCINI and µVerCINI are ideal for imaging anything along the short axes of bacterial cells, as they provide high-resolution images without any special requirements for fluorophores or imaging modalities, and can readily be combined with other imaging methods (e.g. STORM). VerCINI can easily be incorporated into existing projects by researchers with expertise in bacteriology and microscopy. Nanofabrication can be either done in-house, requiring specialist facilities, or outsourced based on this protocol.

## KEY REFERENCES USING THIS PROTOCOL

Bisson-Filho, A. W. et al. *Science* **355**, 739-743 (2017): 10.1126/science.aak9973

Perez, A. J. et al. *Proc. Natl. Acad. Sci.* **116**, 3211-3220 (2019): 10.1073/pnas.1816018116

Whitley, K. D. et al. *Nat. Commun.* **12**, (2021): 10.1038/s41467-021-22526-0

## INTRODUCTION

Although long underappreciated as amorphous sacks of enzymes, it is now clear that bacterial cells are highly spatially organized. How bacterial proteins dynamically organize and remodel large cellular structures such as the cell wall or the chromosome is a central question in bacteriology. However, imaging cellular spatial organisation and dynamics inside bacteria by light microscopy is challenging for several reasons. Firstly, bacteria are very small, with a typical diameter of 1 µm, not much larger than the 250 nm diffraction limit of visible light. Secondly, most bacteria are not spherically symmetric, but exist in a wide range of shapes including rods and ovoids. During imaging, non-spherical bacteria

are usually immobilized flat on a microscope coverslip, with their long axes parallel to the imaging plane and their short axes orthogonal to the imaging plane (Figure 1a, top). Imaging structure and dynamics along the short axes is therefore difficult, both due to a significant amount of background signal from out-of-focus light and the fact that axial resolution is generally lower than lateral resolution (approximately 250 nm lateral vs 550 nm axial resolution[1]).

This is especially problematic when one considers that many bacterial processes occur, or are organized, along these shorter axes. For example, the peptidoglycan cell wall is primarily synthesized circumferentially around the cell during vegetative growth in many bacteria[2–4]. Similarly, when cells divide, their division machinery moves circumferentially around the cell septum to progressively synthesize the cell septum inwards[5,6]. When cells have divided, what was once the division plane becomes two daughter cell poles, which then also exist along the short axes of the cells. A large number of proteins localize specifically to the cell poles in rod-shaped bacteria that carry out a wide variety of functions, such as chemotaxis, motility, adhesion, virulence, chromosome organisation, cell-cycle regulation, and secretion[7–11]. A wealth of information on all these systems has been obtained from microscopy in recent years, but a major limitation remains that the horizontal orientation of cells is far from optimal for imaging these systems.

To address this problem we developed a method, termed Vertical Cell Imaging by Nanostructured Immobilisation (VerCINI), that enables high resolution light microscopy of any process organized along the short axes of bacterial cells by orienting cells vertically in nanofabricated cell traps[5,12,13]. We also developed a method for high-resolution imaging of the short axes of bacteria during fluid exchange termed Microfluidic VerCINI (μVerCINI)[12]. Here we provide a detailed practical guide to implementing both VerCINI and μVerCINI. We first give a general overview of the VerCINI method and its applications. We provide detailed workflows for all aspects of VerCINI and μVerCINI, from nanofabrication of micropillar arrays to acquisition and analysis of microscopy data. We provide rationales for the procedures described and include tips from our own experience in developing and using the methods to assist interested researchers. We also provide quantitative analysis of critical steps in the method to support troubleshooting and to enable future extensions and adaptations of the technique to new applications. By following the procedures described, this article should allow interested researchers to easily apply VerCINI to their own research.

**Development of the protocol**

We recently developed two methods that enable high resolution imaging of bacteria along their short axes by orienting them vertically in nanofabricated cell traps[5,12,13]. In the first method, VerCINI, cells are confined in nanofabricated 'microhole' arrays formed in an agarose pad such that the short axes of the cell are aligned to the microscope imaging plane, allowing much higher resolution images of the cell short axis than is possible with conventional immobilisation (Figures 1a and 2a, bottom). In the second method, termed Microfluidic VerCINI (μVerCINI), the microhole arrays are open-topped, and the vertically trapped cells are confined within a microfluidic chamber to enable rapid solution exchange and chemical perturbation (Figure 3a). Both methods were originally developed to trap rod-shaped bacterial cells, which include the majority of model systems (e.g. *Bacillus subtilis* and *Escherichia coli*) and many human pathogens (e.g. *Mycobacterium tuberculosis*). However, they are suitable for any cells with cylindrical symmetry, which also includes ovococcal species such as the human pathogen *Streptococcus pneumoniae*.

The key principle behind VerCINI is to rotate the short axes of bacteria into the microscope image plane by trapping cells in narrow microholes formed from either agarose or PDMS (Figures 1a, 2a, and 3a). In order to trap cells vertically, a silicon micropillar array serving as a negative master of the microholes

must be fabricated at sufficient resolution for precise and reproducible cell trapping. In standard VerCINI, this micropillar array is used as a mould to form a microhole array in agarose. Bacteria are then immobilized within the traps, imaged using a high-resolution inverted microscope, and data analysed using custom image processing software tailored to maximise SNR of VerCINI microscopy data. µVerCINI uses the same principle as standard VerCINI, but additionally enables rapid drug treatment of trapped cells by immobilizing bacteria in open-topped PDMS cell traps. VerCINI can also be easily combined with denoising, super-resolution microscopy, or single-particle tracking methods to further improve image quality or resolution.

**Advantages and limitations**

VerCINI and µVerCINI offer several benefits for imaging the short axes of cells compared to conventional imaging of horizontally oriented cells:

- *High resolution.* A slice across the plane with the short axes of the cell (e.g. the cell septum) can be viewed at high 250 nm resolution (Figure 1 bottom), rather than just a thin volume of the bottom of the cell (TIRF microscopy, Figure 1 top) or low 550 nm resolution imaging via 3D fluorescence microscopy.
- *Simultaneous imaging of an entire slice of the cell short-axes plane.* An entire slice of the plane with the short axes of the cell can be imaged at once. Proteins that are primarily moving circumferentially, e.g. divisome or elongasome proteins, can then be tracked for extended periods[12], unlike TIRF, which truncates protein trajectories due to its small illumination volume.
- *High signal-to-noise ratio (SNR) imaging of the cell poles.* By rotating cells vertically, the cell pole is placed in contact with/near to the microscope coverslip, and is also oriented to the microscope image plane. This allows high SNR imaging of the cell poles via TIRF illumination, while at the same time improving spatial resolution. Below, we demonstrate proof of concept application of VerCINI to imaging of cell pole protein dynamics (Figure 2).

Limitations to VerCINI and µVerCINI include the following:

- *Incompatible with long or chained cells.* Cells that are filamentous or form long unseparated chains are not likely to fit in the holes. In some cases these issues can be rectified with appropriate genetic modifications: for example, we have found that deleting the *hag* gene (encoding flagellin) or *slrR* gene (encoding a transcriptional regulator[14]) in the *B. subtilis* PY79 background greatly reduces the presence of long unseparated chains of cells, enabling efficient loading into holes[12].
- *Difficult to use with cells lacking cylindrical symmetry.* Although curved cells such as *Caulobacter crescentus* can be loaded into the microholes, data analysis for such cells can be complicated by the fact that the long (curved) axis of the cell is not parallel to the (straight) axis of the microscope, except at the cell mid-plane. One possibility to rectify this may be to first straighten such cells by deleting genes giving them curvature (e.g. *creS* in *C. crescentus*).
- *µVerCINI requires some non-standard microscope parts.* Due to the layer of PDMS between the microscope coverslip and vertically-trapped cells, imaging with this method currently requires a special objective lens and non-standard autofocus system. The specific reasons for this limitation and possible solutions are discussed in further detail in the Experimental Design section.

**Applications**

A key application for VerCINI is imaging the circumferential dynamics of cell division proteins. The septal peptidoglycan synthesis machinery moves circumferentially around the cell to build the cell wall, guided by the essential cytoskeletal protein FtsZ[5,12]. With conventional imaging, the division plane is orthogonal to the microscope imaging plane (Figure 1a, top), and hence the dynamics of division proteins are difficult to observe due to the background signal from out-of-focus light coming from the rest of the division ring. This background signal can be largely removed using total internal reflection fluorescence (TIRF) illumination, which produces an evanescent wave that excites only the bottom 100-200 nm of the cell, but this limits imaging to only a small slice of the division septum (Figure 1b-c, top). In contrast, VerCINI allows simultaneous imaging of the entire septum, and strongly reduces background signal, because the septum no longer overlaps itself axially.

Using an early prototype of VerCINI, we observed the circumferential dynamics of FtsZ of the model rod-shaped *Bacillus subtilis* around the full division ring at high resolution and discovered that FtsZ filaments treadmill in the living cell (Figure 1b-c, bottom)[5]. VerCINI has since found a variety of applications in cell division microscopy. Using an optimized version of VerCINI with increased SNR, we were able to image FtsZ dynamics at near-single-filament resolution throughout the *B. subtilis* division cycle, demonstrating that FtsZ filament condensation into a dense Z-ring drives a transition in FtsZ dynamics from a mixed population of mobile and immobile filaments to stable treadmilling during constriction initiation and active septum building. With µVerCINI we were also able to demonstrate that the FtsZ-targeting antibiotic PC190723 totally arrests FtsZ filament motion within seconds (Figure 3b-c). Beyond this, VerCINI has been applied to image division in several different bacterial species using a variety of imaging methods: the dynamics of FtsZ treadmilling in the ovococcoid bacterial pathogen *Streptococcus pneumoniae*[13], the organisation of FtsZ and FtsN in *Escherichia coli* using STED super-resolution imaging[15], the division-associated cell wall synthase FtsI in *E. coli* using single-particle tracking[16], and peptidoglycan synthesis during division and elongation in *S. pneumoniae* using dSTORM with fluorescently-labelled 'clickable' D-amino acids[17].

VerCINI also has multiple applications to cellular systems beyond cell division. Since the cell wall is synthesized circumferentially in many bacteria, nearly any protein involved in these processes is an ideal candidate for investigation with VerCINI. For example, we are currently using single-particle tracking to image the circumferential motion of the elongation-associated cytoskeletal protein MreB in *B. subtilis* (unpublished). Another possible application of VerCINI is the bacterial nucleoid and associated proteins, which may show significant radial organisation due to the combined effects of transcription and translation[18]. The general concept of using vertical cell immobilisation to improve imaging resolution has also been applied successfully to eukaryotic systems, although both the microfabrication and microscopy approaches required there differ substantially due to the much larger cell size[19–21].

We believe that a major potential application of VerCINI is the imaging of cell poles. Vertical orientation increases the spatial resolution of cell pole organisation, and high signal-to-noise imaging with TIRF illumination becomes uniquely possible as the cell pole is placed in contact with the microscope coverslip. To illustrate this we provide brief proof-of-concept demonstration of VerCINI to cell pole imaging by investigating the dynamics of the *B. subtilis* chemoreceptor protein TlpA (Figure 2; Supplementary Methods). TlpA is a chemoreceptor protein in *B. subtilis* that forms large clusters localized to both the base of division septa and cell poles (Figure 2a-b), likely due to a binding preference for regions of high membrane curvature[22]. With conventional imaging, the distribution and dynamics of these clusters are obscured by the signal from overlapping clusters (Figure 2b, top). In contrast, orienting cells vertically with VerCINI and illuminating via TIRF allows for high resolution, high SNR imaging of these clusters at cell poles (Figure 2b-d). We observed that TlpA forms multiple large,

essentially immobile clusters (generalized diffusion coefficient $\langle K_\alpha \rangle = 5 \cdot 10^{-7} \pm 6 \cdot 10^{-7}$ μm$^2$/s$^\alpha$ (mean ± SD) for the data shown in Figure 2) of varying size, consistent with large chemoreceptor arrays observed in other organisms by cryo-electron tomography[23] (Figure 2b-d, bottom).

This protocol was optimised using *B. subtilis* strain PY79, although it is applicable to a wide range of bacterial cell types. We have used it to image *B. subtilis* 168, *S. pneumoniae* D39[13], *Corynebacterium glutamicum* RES 167, and *E. coli* MG1655 while others have used it to image *S. pneumoniae* strain R800[17]. This protocol should be generally applicable to any bacterial cell type with cylindrical symmetry. Preliminary VerCINI measurements of the curved, non-cylindrical *Caulobacter crescentus* also gave successfully trapped cells, indicating that VerCINI may be also applicable to other curved rod-like cells.

**Experimental design**

**Nanofabrication of micropillars.**

We use e-beam lithography and deep reactive ion etching (DRIE) to create the micropillars on a silicon wafer using an approach similar to Deshpande & Dekker (2018)[24].

We designed square microholes, as we hypothesized that a deformable material like agarose should trap cells more efficiently than circular ones due to a small number of cell-microhole contact points, leading to a larger fit tolerance. The following protocol is therefore for an array-of-squares pillar pattern (Figure 4c).

Since each silicon wafer can easily be split into four quarters, we recommend making four identical patterns—one in each quadrant (Figure 4c)—to maximise the utility of the wafer. Although space is available on the wafer to accommodate larger arrays, we use an overall pattern size of ~1 × 0.5 cm$^2$ because the agarose pad that will eventually contain this pattern will need to be cut down prior to imaging to ensure sufficient oxygen delivery to trapped cells (see Figure 6avi).

When using VerCINI for the first time, we recommend making several columns of differently-sized pillars (Figure 4c) to later find the optimal size for your particular bacteria and growth conditions (for *B. subtilis* we have found that pillars of width 1.0-1.3 μm work best). Importantly, we have found that the Bosch etching process shrinks the squares substantially (Figure 5a-b) from the designed widths due to some degree of 'isotropic etching' (i.e. undercutting the resist), and so the designed widths must be larger to compensate. The amount that pillars shrink during the Bosch etch depends on both the sizes of gaps between pillars (Figure 5c) and the duration of the Bosch etch. For gaps of 3.0-3.5 μm, we have measured a decrease in widths of 560 ± 110 μm (mean ± SD) for a 100 s Bosch etch (N=4 wafers) and 680 ± 40 μm (mean ± SD) for a 140 s Bosch etch (N=2 wafers). However, for a given gap size and Bosch etch time, we have found that the decrease in pillar widths is reproducible.

One other critical factor when designing the array-of-squares pattern is e-beam write time. Since it takes significantly more time for the e-beam system to move the sample stage than to deflect the beam, moving the stage to write each individual square shape will require a prohibitively long amount of time. However, the area over which the e-beam can write at a single stage position (the main field; ~1×10$^6$ μm$^2$ for our Raith EBPG-5000+) is much larger than each individual square that will be written (~1 μm$^2$). So, the protocol below describes how to produce an array of squares that is roughly the same size as the e-beam's main field, and then later replicate this array to obtain a larger array pattern. This way, thousands of squares are written at each stage position, dramatically reducing the e-beam write time.

One further consideration is the heights of pillars that will be needed. The optimal heights are mainly determined by the average length of cells that users want to eventually image in microholes (for *B. subtilis* we typically use pillars of height 4-7 µm). Pillars can also be made taller to accommodate longer cells or multiple short cells as a column, but taller (i.e. higher aspect ratio) pillars are more fragile and susceptible to breaking when agarose or polydimethylsiloxane (PDMS) are peeled off of them. We have successfully used pillars with aspect ratio up to ~10 (1 µm square pillars 10 µm tall), but it is likely that pillars with much higher aspect ratios will not be feasible. To further prevent pillars breaking when PDMS is peeled off, we coat the wafers with a silane compound (tridecafluoro-1,1,2,2-tetrahydrooctyl trichlorosilane) by vapour deposition to prevent strong adhesion. Although designed to enable solidified PDMS to be removed, we also found that this silane coat makes solidified agarose peel off more easily as well.

For researchers that do not have access to a nanofabrication facility, silicon wafers for VerCINI can be fabricated commercially based on this protocol. We are currently performing prototyping and testing with ConScience AB, Sweden, to make VerCINI chips available to other researchers, without financial benefit to ourselves. ConScience have estimated production cost at $2900 per wafer ($700 per VerCINI chip). The authors or the company may be contacted for updates. Other companies should also be able to fabricate these devices.

**Sample preparation and imaging**

To image cells during vegetative growth, VerCINI pads are made using agarose dissolved in growth media using an approach adapted from de Jong et al. (2011)[25]. The porous nature of the agarose gel allows nutrients to diffuse through to cells allowing continued growth during the imaging process, while a high agarose concentration makes the gel stiff, providing structural stability to the microholes.

One critical factor for VerCINI is the efficiency with which cells are loaded into holes. A higher loading efficiency corresponds to more trapped cells in a single FoV, and therefore greater data acquisition. We have found that centrifuging concentrated cell culture into the holes using a flat bottomed centrifuge rotor gives high loading efficiency (Figure 6c-d).

Another important consideration is that cells are sometimes poorly trapped in the holes, causing them to wobble (Supplementary Video 1). Although these are relatively rare for correctly sized micropillars, imperfectly-trapped cells can be identified and removed from further analysis by recording a short (~1 s) bright-field video after fluorescence acquisition. We initially hypothesized that flagellar motility might cause this poor trapping. However, at least in *B. subtilis* this does not appear to be the case, as deleting the *hag* gene made little difference to the amount of poorly trapped cells. In the less chain-forming *B. subtilis* strain BS168 we frequently perform experiments in motility-proficient cells without issue.

After loading, cells can be imaged using any microscope technique suitable for studying bacterial spatial organisation. Importantly, microholes are imprinted on the top of the agarose pad, so the cells are adjacent to the coverslip surface (Figures 1b and 2b). This means that illumination techniques such as HILO (for cell sidewall; e.g. Figure 1b) and TIRF (for cell poles; e.g. Figure 2b) are preferable to maximize image signal to noise ratio (SNR). We employ a ring-TIRF or ring-HILO system, where galvanometer-driven mirrors rotate the illumination beam at high speed (200 Hz) to produce uniform illumination across the sample[26], however single angle TIRF or HILO are also sufficient.

**µVerCINI**

In many experiments, researchers want to perform rapid solution exchange during imaging, either to change from one medium to another, to add perturbatives such as antibiotics, to fix cells, or to label cells with exogenous dyes. However, with the original VerCINI method this is not possible since the slide is closed and the cells are underneath a dense pad of agarose. We have therefore designed an adapted version of the method to be compatible with solution exchange, called microfluidic VerCINI (µVerCINI). In this method, the microholes are open-topped (Figure 3a), and the cells are exposed to a fluid environment that is controlled by users through a microfluidic system.

One critical difference with this open-topped orientation is that there is a layer of material between the coverslip surface and the cells through which imaging will be done. Making a thin layer with agarose is challenging, and imaging through a thick layer of agarose would lead to substantial loss in image quality due to scattering. We instead use PDMS, which forms a relatively thin (~50 µm) transparent layer (Figure 7a).

Because the holes are formed of PDMS rather than agarose, loading cells into the holes of a µVerCINI coverslip differs somewhat from VerCINI. PDMS is normally quite hydrophobic, and the surface tension of an aqueous cell culture is high enough that the microholes will end up filled with air bubbles rather than liquid or cells. PDMS is therefore first rendered hydrophilic by treatment with oxygen or air plasma (Figure 7ci).

After cells are loaded, the µVerCINI coverslip is adhered to a pre-fabricated device (Figure 7b) to form a closed microfluidic chamber (Figure 7d). This device consists of a microscope slide with drilled holes to allow for inlet and outlet tubing, along with a piece of double-sided tape that has been cut to form a flow channel. The double-sided tape serves two functions: it forms a thin (~100 µm) flow channel between the microscope slide and the tops of the microholes, and it seals the whole system together. It is important to identify a suitable double-sided tape as not all brands of double-sided tape adhere well to PDMS, which can produce leaks. We have found that Duck and Club brand double-sided tapes work well, while Scotch, Sellotape, and WHSmith double-sided tapes do not.

There are two key points to consider when imaging with µVerCINI. Firstly, even with a relatively thin 50 µm PDMS layer on top of a #1.5 microscope coverslip we found that we cannot successfully acquire images using a high N.A. oil immersion 100x TIRF objective. This is likely due to spherical aberration resulting from refractive index mismatch between PDMS ($n$=1.43) and glass ($n$=1.52). We instead use a silicone immersion oil objective since the silicone oil refractive index ($n$=1.41) is similar to PDMS. This objective also has a large working distance (0.3 mm) which is useful for imaging through the PDMS layer.

Secondly, µVerCINI is not compatible with reflection-based autofocus systems. This is because very little reflection occurs off the PDMS/liquid interface, as the indices of refraction are too similar (~1.43 and ~1.33, respectively). One possible solution is to use image-based autofocus methods (e.g. Micro-Manager's OughtaFocus), however these are not suitable for correcting drift during high-speed imaging of protein dynamics. A solution that we favour is to use an image-based autofocus system that measures drift using the cross-correlation between images and a reference stack in a separate infrared bright-field illumination and imaging pathway[27]. We developed a custom plugin for Micro-Manager to set the reference stack, calculate the cross-correlation maps, and maintain sample focus by closed-loop positioning of the microscope stage[12]. We perform the IR drift correction method on a custom built high resolution microscope, but the apparatus for this method can also be retrofitted onto commercial microscopes[27]. If automated drift correction methods are not available, with practise it is possible for a skilled operator to continuously manually correct for drift during image acquisition.

However, this will usually lead to reduced image quality due to increased periods of defocus during data acquisition.

It is also important to note that—unlike VerCINI—µVerCINI is often used for 'single-shot' experiments, which limits users to recording a single field of view. For example, if a researcher wants to image the effect of an antibiotic perturbation on protein dynamics inside cells (e.g. Figure 3c), then the experiment can't be repeated on a different field of view with the same slide, as all cells on the slide have already been perturbed. Because of this it is imperative not only to have high loading efficiency, but also to take some time to scan across the slide and find the best possible field of view before beginning.

**Image processing and analysis**

We focus here on our most common VerCINI image analysis use case: analysis of protein motion around the cell circumference or cell septum via kymograph analysis. This analysis method is appropriate when protein motion is mostly restricted to the leading edge of the cell septum (e.g. FtsZ) or the cell sidewall (e.g. MreB or other elongasome proteins). For other datasets, such as TIRF imaging of cell pole-localized proteins, other analysis methods such as single molecule tracking may be more appropriate. The overall workflow for image processing and analysis is shown in Figure 8a.

The first steps of image processing are done in Fiji/ImageJ[28]. We have developed a plugin called VerciniAnalysisJ specifically for processing VerCINI videos, which can be installed from the VerciniAnalysisJ update site with all its dependencies. Later image processing steps such as subtracting the cytoplasmic background signal and producing kymographs are done in MATLAB. We have developed software for these steps in a package called ring-fitting2 that is publicly available on GitHub[29].

Two key processing steps are image denoising and registration. We found that image denoising allows us to substantially reduce illumination intensity while still maintaining high signal to noise ratio, thereby minimizing photobleaching and phototoxicity. We strongly recommend denoising VerCINI data prior to subsequent analysis. While a number of denoising algorithms have been developed, we use the ImageJ plugin PureDenoise, which is based on wavelet decomposition[30]. One advantage to using this algorithm is that it does not make any assumptions about the underlying biological structure. After denoising, any global image drift—for example due to agarose contraction—is corrected via image registration using the ImageJ plugin StackReg[31].

Our *ring-fitting2* software automatically extracts kymographs of circumferentially localised protein dynamics[12] (Figure 8d-e). This software also subtracts the diffuse out-of-focus cytoplasmic background (Figure 8d), which can otherwise obscure protein dynamics. The background signal is subtracted from the image stack for each frame, and then the intensity around the fitted circle is calculated to sub-pixel precision via interpolation. We found that sub-pixel fitting of the cell centre and septum/ circumference and robust background subtraction were crucial to obtaining accurate intensity measurements. During software development, we observed that small inaccuracies in cell centre localisation, caused for example by fitting an annulus with uniform instead of sectored amplitude would cause large errors in apparent septal intensity as the small size of the cell, together with the complex background meant that different amounts of background signal would be integrated on either side of the cell. In order to confirm that the microscope system and image processing pipeline are together giving even circular symmetric intensity measurements around the centre of the cell, a cell expressing cytoplasmic GFP can be imaged and analysed. An example script for this purpose is supplied in the VerCINI analysis software.

Processive protein motion is visible on kymographs as a diagonal line, with line angle indicating protein speed. For dense protein filaments such as FtsZ, we currently quantify protein speed, bound lifetime, and other parameters such as directional switching and pausing by manual kymograph annotation (Figure 8g-h), as we found that most automated kymograph annotation methods do not perform well at high density. An ImageJ macro is provided for quantification of filament dynamics via manual ImageJ regions of interest (ROIs) annotation. During kymograph analysis, it can be difficult to identify trajectories of dim filaments due to the large intensity range within kymographs. This issue is frequently encountered for analysis of FtsZ dynamics in dense Z-rings. To address this issue, we recommend applying a ridge detection filter to the kymograph, which detects peaks within an image irrespective of intensity based on the image second derivative. A script *'Ridge_Filter.ijm'* is provided for this purpose. We note that a recent deep learning based kymograph annotation tool could enable automated processing of VerCINI kymographs in the future[32].

**Level of expertise needed to implement the protocol**

The nanofabrication protocol we describe to obtain a micropillar silicon wafer requires a cleanroom facility with appropriate training. This requirement can be avoided by ordering commercially fabricated wafers. Once a micropillar wafer is available, the rest of the VerCINI/µVerCINI protocol can be performed in any bacteriology lab with expertise in live single cell resolution fluorescence microscopy. Although µVerCINI does not require prior expertise in soft lithography or microfluidics, it is more difficult than VerCINI due to some specialized hardware and more complicated assembly. We therefore recommend users to become experienced at using VerCINI prior to trying µVerCINI.

# MATERIALS

## REAGENTS

- Silicon wafer (4-inch diameter, 500 µm thickness, one side polished, type/orientation NP<100>, PB<100>, resistivity 1-10 Ω·cm; International Wafer Service)
- 1,1,1,3,3,3-hexamethyldisilazane (HMDS; VWR, cat. no. 51152885). CAUTION: This compound is highly flammable and is toxic on contact with skin or if inhaled. Wear protective gloves, protective clothing, eye protection, and face protection.
- Negative e-beam resist (e.g. AR-N-7700.18; Allresist)
- Developer (e.g. Microposit MF-321; micro resist technology)
- (Tridecafluoro-1,1,2,2-tetrahydrooctyl)tricholorosilane (abcr, cat. no. AB111444). CAUTION: This compound is flammable, and causes severe skin burns and eye damage. It reacts with water to produce hydrogen chloride. Wear protective gloves, protective clothing, eye protection, and face protection. Work in a dry, inert gas atmosphere while handling. Once aliquoted, flush the stock bottle with argon and seal the lid with parafilm.
- Ultrapure agarose (Invitrogen, cat. no. 16500-100)
- Polydimethylsiloxane (PDMS) elastomer base (Dow Corning, Sylgard 184 elastomer base)
- PDMS curing agent (Dow Corning, Sylgard 184 elastomer curing agent)
- Cell growth media (experiment-specific, but ideally should have low autofluorescence)

## BIOLOGICAL MATERIALS

- *B. subtilis* SH130 (PY79 Δ*hag ftsZ*::*ftsZ-gfp-cam*)[12].
- *B. subtilis* HS48 (168 *amyE::spc* $P_{xyl}$-*tlpA-mgfp*)[22].

## EQUIPMENT

### Cleanroom equipment

- Spin-coating system (SUSS MicroTec)
- Hot plates (Harry Gestigkeit, cat. no. 2860EB)
- Syringe (5 mL; e.g. BD Plastipak)
- Syringe filter (0.22 µm; e.g. Starlab)
- Electron-beam lithography system (Raith, model no. EBPG5000+)
- Upright microscope (Olympus, model no. BX51M)
- Deep reactive ion etching system (Adixen; AMS, model no. 100 I-speeder)
- Stylus profilometer (Bruker, model DektakXT)
- Scanning electron microscope (e.g. FEI, NovaNano SEM)

### Wet lab equipment

- Inert gas (e.g. argon) supply
- Vacuum desiccator (Kartell)
- Vacuum pump (Leybold Trivac, model no. D8B)
- Diamond scribe (e.g. RS Pro, Stock No. 394-217)
- Gene Frames (65 µL, 1.5 × 1.6 $cm^2$; Thermo Scientific)
- Microwave
- Water bath with heater (e.g. Grant, model JB Nova)
- Mini-centrifuge (Eppendorf, model 5424)
- Silicone gaskets (Sigma-Aldrich, cat no. GBL103240), cut into individual 9 mm gaskets
- Centrifuge (VWR, model 5810, cat. no. EPPE5810000.060)
- Rotor with flat-bottomed buckets (VWR, A-4-81 Swing-out Rotor with 4 x MTP/Flex Buckets, cat. no. 521-0145)
- Oven (e.g. Falc Instruments, Mini Oven STZ 5.4)
- Flat blade (e.g. Stanley 18 mm snap off blades, cat. no. 0-11-301)
- Power drill (e.g. Dremel, Dremel 4000)
- Multi-chuck for power drill (e.g. Dremel, 0.8-3.2 mm keyless chuck)
- Diamond-tipped drill bits (0.75 mm; Kingsley North, cat. no. 1-0500-100)
- Double-sided tape (e.g. Duck, 38 mm × 5 m)
- Pipette tips (e.g. Starlab, 10 µL)
- Polyethylene tubing (ID 0.38 mm, OD 1.09 mm; Smiths Medical, cat. no. 800/100/120)
- Rapid-drying epoxy (Araldite)
- Needles (0.45 mm × 10 mm (26g x 3/8”); BD Microlance)
- Plasma cleaner (Harrick Plasma, cat. no. PDC-002-CE)
- Syringe (20 mL; BD Plastipak)
- Syringe pump (Aladdin-220; World Precision Instruments)

### Microscopy equipment

- Microscope slides (e.g. VWR Super Premium)
- Microscope coverslips (22 × 22 $mm^2$, thickness no. 1.5; VWR)
- Inverted fluorescence microscope, preferably with laser-based total internal reflection fluorescence (TIRF)/ highly inclined and laminated optical sheet (HILO) illumination (e.g. Nikon N-STORM).

- 100× oil immersion objective (e.g. Nikon, CFI Apochromat TIRF 100XC Oil)
- 100× silicone oil immersion objective (Nikon, CFI SR HP Plan Apo Lambda S 100XC Sil, for µVerCINI only)
- Microscope incubation or stage heating device (for live cell microscopy)

**SOFTWARE**

- Computer-aided design (CAD) software (e.g. AutoCAD (Autodesk), https://www.autodesk.eu/products/autocad/overview)
- BEAMER (GenISys, https://www.genisys-gmbh.com/beamer.html)
- Cjob (Vistec Lithography)
- Image acquisition software (e.g. Micro-Manager v2.0gamma, https://micro-manager.org/)
- Fiji v1.53 (https://fiji.sc)
- VerciniAnalysis ImageJ plugin (https://github.com/HoldenLab/VerciniAnalysisJ)
- MATLAB (Mathworks)
- ring-fitting2 MATLAB package (https://github.com/HoldenLab/ring-fitting2)

# PROCEDURE

**Design of an array-of-squares pattern. TIMING ~30 min – 2 hr**

1. Make a 1 × 1 µm$^2$ square in AutoCAD. Save it as a dxf file.
2. In BEAMER, make an array of squares the size of the e-beam main field. One possible algorithm to achieve this is shown in Figure 4a.
   a. Input the dxf file containing the square.
   b. Use one loop to scale the square to a range of different sizes, as desired (e.g. 1.4-2.0 µm edge lengths).
   c. Within this loop, use two more loops in series to make an array of squares in X and Y, selecting the option to merge the results of all loops rather than to only keep the final loop iteration. Arrays of each desired square size will be output as a separate gpf file. **?TROUBLESHOOTING.**
3. In Cjob, load the gpf files from BEAMER and replicate them several times to make four full arrays, one in each quadrant of the wafer. Also add in identifiers and a solid rectangle to measure heights. A code structure to achieve this is shown in Figure 4b.
   a. For Substrate, choose a 100 mm diameter silicon wafer and 100 kV exposure.
   b. Using Layout, replicate all patterns in each quadrant of the wafer to maximize its use (2×2).
   c. Again using Layout, replicate the gpf files from BEAMER to make a large array pattern in each wafer quadrant. We repeat the pattern 2× in the X direction and 5× in the Y direction. Select the following parameters for writing: dose = 117 µC/cm$^2$ (for AR-N-7700 resist), beam step size = 25 nm, beam size = 56 nm.
   d. Add identifiers around the entire array so that the sizes can be identified later under a microscope. Select the following parameters for writing: dose = 117 µC/cm$^2$, beam step size = 50 nm, beam size = 95 nm.
   e. Add a solid 1000 × 500 µm$^2$ rectangle above each array so that the heights can be measured with a profilometer after etching. Write the rectangle with the parameters: dose = 117 µC/cm$^2$, beam step size = 50 nm, beam size = 95 nm.
   f. Export the file as a job to the e-beam system.

**Fabrication of a silicon micropillar wafer. TIMING ~3 hr**

**CRITICAL:** Steps 4-10 should be performed in a cleanroom facility (for this work, a class 10,000 (International Organization for Standardization (ISO) 7) facility with a class 100 (ISO 5) work area was used). These steps are adapted from Deshpande & Dekker (2018)[24].

4. Spin-coat the wafer with negative e-beam resist.
    a. Prime a 4-inch diameter silicon wafer by spreading ~5 mL HMDS on the polished side, and spin-coating it at 1000 rpm for 1 min. Immediately bake the wafer at 200°C for 2 min. HMDS will increase adhesion of the resist. (Prior to spin-coating, the wafer can optionally be cleaned with fuming nitric acid to remove dust and impurities. This is recommended to prevent non-uniform deposition of resist on the wafer during spin-coating and hence ensure that the patterns avoid defects arising from this. However, we have found that this step is typically unnecessary if fresh silicon wafers are used straight from packaging.)
    b. Using a 0.22 µm filter, carefully spread ~5 mL of AR-N-7700.18 resist on the wafer. If bubbles appear, gently move them away from regions where patterns will be written using either the tip of the syringe filter or a cleanroom wipe. Spin-coat the wafer at 500 rpm for 1 min, then immediately bake at 85°C for 2 min. **?TROUBLESHOOTING.**
5. Write the array-of-squares micropillar pattern on the coated wafer using an electron-beam lithography system following the manufacturer's instructions.
6. Bake the wafer immediately after writing at 105°C for 2 min. **CRITICAL STEP:** Failure to bake the wafer will result in patterned region dissolving during development. **PAUSE POINT:** The baked wafer can be kept at room temperature (~22°C) in a dust-free environment indefinitely.
7. Develop the wafer to remove the resist that was not exposed to the e-beam.
    a. Soak the wafer in MF-321 for 90 s and swirl gently.
    b. Immediately, soak the wafer in diluted MF-321 solution (10% v/v MF-321 in water) for 30 s and swirl gently.
    c. Immediately, soak the wafer in water for at least 30 s, swirling gently.
    d. Dry the wafer.
    e. Inspect the wafer under an upright light microscope at 60-100× magnification to ensure patterns have developed properly. **PAUSE POINT:** The developed wafer can be kept at room temperature in a dust-free environment indefinitely. **?TROUBLESHOOTING.**
8. Etch the wafer using a Bosch process in an AMS 100 I-Speeder to produce vertical pillars, then remove the remaining resist with $O_2$ plasma.
    a. Clean the chamber of the inductively coupled plasma (ICP) reactive ion etcher for 20 min prior to beginning. Using $O_2$ gas set to 200 standard cubic centimeters per min (SCCM) with ICP power set to 1800 W and biased power set to 60 W.
    b. Place the wafer in the etcher and set the following parameters: wafer temperature = 10°C, chamber pressure = 0.04 mbar, source-target distance = 200 mm.
    c. Etch the wafer using a Bosch process. The etching step is 200 SCCM $SF_6$ for 7 s with ICP power set to 2000 W and capacitive coupled plasma (CCP) power at 0 W. The passivation step is 80 SCCM $C_4F_8$ for 3 s with ICP power set to 2000 W and CCP power in chopped low-frequency bias mode: 80 W for 10 ms and 0 W for 90 ms. The etching time depends on the desired structure height (see Figure 5d for guide).
    d. Remove the resist with the AMS 100 I-speeder using $O_2$ gas at 200 SCCM for 10 min with the following parameters: wafer temperature = 10°C, chamber pressure = 0.04 mbar, source-target distance = 200 mm, ICP power = 2500 W with biased power = 50 W.
9. Measure the height of the etched structures by moving the stylus of a DektakXT profilometer over the 1000 × 500 $\mu m^2$ rectangle in the pattern.

10. Inspect the true widths of the pillars with a scanning electron microscope. **PAUSE POINT:** The silicon wafer can be kept at room temperature indefinitely.

**Passivation and dicing of the silicon micropillar wafer. TIMING ~12 hr**

11. Passivate the silicon micropillar wafer with a silane compound using vapour deposition.
    a. Evacuate air in a glass desiccator with argon to remove moisture.
    b. Pipette 10 µL of (tridecafluoro-1,1,2,2-tetrahydrooctyl)trichlorosilane into a tube in the desiccator. Leave the tube open.
    c. Place the wafer in the desiccator. Pull vacuum in desiccator down to ~10 mbar.
    d. Close the desiccator valve and turn off the vacuum.
    e. Remove wafer after ~12 hr. **PAUSE POINT:** The silanized wafer can be kept at room temperature indefinitely.
12. (Optional) Split the wafer into four quarters by scratching with a diamond scribe. Since the wafers are made of a lattice crystal of silicon, they will break along a well-defined plane.

*Sample preparation and imaging protocols for VerCINI (Option A) and µVerCINI (Option B) are described separately. VerCINI imaging using cells immobilized in agarose cell traps (Option A) is the more common use case, and is straightforward to implement. µVerCINI (Option B) is more difficult due to more elaborate sample preparation and imaging, and reduced cell loading efficiency, and should only be attempted after users are experienced at standard VerCINI.*

**OPTION A: VerCINI sample preparation and imaging**

**A.1 Preparation of VerCINI pads. TIMING ~20 – 40 min**

13. Apply a Gene Frame to a microscope slide. Leave the plastic cover adhered to the Gene Frame that has a square hole in the middle.
14. Prepare 10 mL of 6% (w/v) agarose in growth media (with any inducers required) and microwave until dissolved. Short bursts in the microwave with swirling in between allow bubbles to settle.
15. After agarose is fully dissolved, place the molten agarose in a 90°C water bath for 5-10 min. Since the 6% molten agarose is very viscous, this will allow time for bubbles to migrate to the surface while not allowing the agarose to solidify.
16. Using wide-bore pipette tips (or cutting the ends off regular ones), apply 800 µL agarose to the centre of the pillars (Figure 6ai).
17. Gently but firmly press the microscope slide on top of the agarose (Gene Frame down), aligning the micropillars with the centre of the Gene Frame (Figure 6aii). Keep the wafer with attached slide at the temperature at which cells will be imaged. **PAUSE POINT:** Agarose pads should be left in place on the wafer at the imaging temperature until ready to load with cells. **?TROUBLESHOOTING.**

**A.2 Loading cells into VerCINI pads. TIMING ~10 – 20 min**

**CRITICAL:** Steps 18-26 should be performed at a constant temperature as much as possible to avoid perturbations to cell physiology.

18. Centrifuge 0.5-1 mL of cell culture ($OD_{600}$ between 0.3 and 0.5) at 17,000 rcf for 1 min. Concentration and volume of cells added can be adjusted as required.
19. Remove supernatant and resuspend in 8-15 µL pre-warmed media.
20. Using a scalpel, remove agarose slide from the micropillar wafer (Figure 6aiii). To do this, slide the scalpel between the agarose pad and the wafer, then use the scalpel to lever the agarose pad and slide away from the wafer. Take care not to disturb the holes or to touch the nanofabricated pillars. **?TROUBLESHOOTING.**

21. Place a 9 mm silicone gasket on top of the microholes and spot the concentrated cell culture into the centre (Figure 6aiv). To prevent evaporation, cover the gasket with a plastic slip and tape it down to the slide. For this we commonly use the plastic coverslips supplied with Gene Frames, although many other such covers are possible.
22. Tape the slide to a flat-bottomed centrifuge rotor with appropriate balance, and centrifuge at 3,220 rcf for 4 minutes (Figure 6aiv). **?TROUBLESHOOTING.**
23. Wash off excess cells from the top of the pad by holding the pad near-vertically over a waste container (Figure 6av) and slowly (1 mL/5 s) pipetting fresh, pre-warmed media onto the top of the agarose pad, allowing the media to flow over the imprinted area and drop into the waste container. Repeat this step at least 5 times until the majority of excess cells are removed (it is impossible to remove all of the cells so some excess will still be visible by eye). This step is the most inconsistent, so can be adjusted through trial and error. **CRITICAL STEP:** If the washing step is not thorough enough, the pad will be covered in horizontal cells covering up the vertically immobilized cells (Figure 6b). If the pad is washed too aggressively, the vertically immobilized cells will be flushed out of the microholes. The washing step is also important to maintain hydration of the pad after centrifugation.
24. Allow the pad to air dry until no excess liquid remains (~2 min).
25. Remove agarose outside the imprinted region by cutting around the imprinted region using a scalpel. This ensures sufficient oxygen supply to the cells once the coverslip is applied (Figure 6avi).
26. Peel off the remaining plastic from the Gene Frame and apply the coverslip. Ensure the coverslip is fully adhered to the Gene Frame by pressing down around all the edges.

**A.3 Imaging with VerCINI. TIMING 10 min – 12 hr**

**CRITICAL:** If doing live-cell imaging, Steps 27-33 should be done with a microscope that is surrounded by an incubation box pre-heated to the cell growth temperature. Failure to do so can result in temperature shock to the cells, compromising results.

27. Transport the slide to the microscope in a pre-warmed empty pipette tip box to reduce temperature fluctuations in the sample.
28. Mount the slide on the microscope, preferably with a low autofluorescence immersion oil such as Olympus Type-F.
29. Using brightfield illumination, identify an area of the VerCINI slide with a high loading efficiency and a low number of horizontal cells on top of the pad. **?TROUBLESHOOTING.**
30. Using fluorescence microscopy, take snapshots to scan the Z-plane to find the structure you wish to image. Keep the number of snapshots to a minimum to avoid photobleaching. It is often useful to take a Z-stack image of the entire cell to ensure the correct structure and plane are imaged.
31. Set focus lock to the optimal Z-plane.
32. Record a short brightfield time lapse as a control. This allows later identification of wobbling cells which can affect apparent protein dynamics. We recommend recording ~20 frames over ~1 s.
33. Record fluorescence with desired settings.

**OPTION B: µVerCINI sample preparation and imaging (ADVANCED)**

**B.1 Preparation of µVerCINI device. TIMING ~2 hr**

34. Make a 10:1 ratio of PDMS elastomer base : curing agent by mixing 10 g elastomer base and 1 g curing agent in a glass or plastic vessel, and stir vigorously.
35. Degas the mixture by placing it in a vacuum chamber and pulling vacuum for ~15 min.
36. Pour ~1 mL on top of the silicon micropillars (Figure 7ai).
37. Place a microscope coverslip on top and press down gently but firmly with a marker cap similar device with a flat face (Figure 7aii). It is important to press down with enough force to produce a thin layer of PDMS between the pillars and the coverslip, but not so hard that the pillars may be

damaged. Cover the back of the coverslip with some remaining PDMS. This will make it easier to remove some PDMS after baking.

38. Set the silicon wafer with PDMS and coverslip in an oven and bake at 80°C for 1-2 hrs.
39. Take the wafer out of the oven and peel off the outer layer of PDMS covering and surrounding the coverslip. Use a flat-edged blade, such as the bare blade of a utility knife, to slide under and pull off the PDMS-covered coverslip (Figure 7aiii). Be very careful not to damage the pillars with the blade while doing this. **PAUSE POINT:** After fabrication, µVerCINI coverslips can be stored at room temperature indefinitely. **?TROUBLESHOOTING.**
40. Drill two holes in a glass microscope slide ~15 mm apart diagonally using a power drill equipped with diamond drill bits. Use a small volume of water to prevent glass dust kicking up during drilling.
41. Clean the slide to remove glass dust and other impurities by sonicating in ethanol for 15 min and wiping with a tissue.
42. Using either a laser engraver or a blade, cut a groove in a piece of double-sided tape to form the flow channel. The channel must be long enough to reach the inlet and outlet holes, and wide enough in the centre to accommodate the microhole array.
43. Adhere the piece of tape to the microscope slide so that the holes line up with the ends of the channel (Figure 7b). Ensure that the tape seals well by pressing around all the edges. Do not remove the plastic covering from the other side of the tape.
44. Take two 10 µL pipette tips and cut them in half, keeping the thinnest end. Cut a further ~2-3 mm from the ends of the tips (where they are thinnest). We find this prevents the tips from protruding too far through the drilled holes and interfering with fluid flow.
45. Cut two polyethylene tubes for inlet and outlet tubing. We use 24 cm for the inlet and 67 cm for the outlet.
46. Insert the inlet and outlet tubing into the cut pipette tips (Figure 7b) and epoxy them in place.
47. Insert the cut pipette tips into the drilled holes of the microscope slide on the opposite side from the double-sided tape (Figure 7b). Ensure that they do not protrude through the holes. Seal the interface by spreading epoxy between the tip and slide.
48. Slide a needle into the outlet tubing entrance. **PAUSE POINT:** The microfluidic chamber top can be stored at room temperature indefinitely. **?TROUBLESHOOTING.**

**B.2 Loading cells into µVerCINI coverslip. TIMING ~10 – 20 min**

**CRITICAL:** Steps 49-57 should be performed at a constant temperature as much as possible to avoid perturbations to cell physiology.

49. Treat the PDMS-coated coverslip with air or oxygen plasma for 3 min (Figure 7ci). This treatment renders the PDMS hydrophilic for a relatively short time (a few hours), as material deeper in the PDMS will eventually migrate to the surface and render it hydrophobic again.
50. Centrifuge 0.5-1 mL of cell culture ($OD_{600}$ between 0.3 and 0.5) at 17,000 rcf for 1 min. Concentration and volume of cells added can be adjusted as required.
51. Remove supernatant and resuspend in 8-15 µL pre-warmed media.
52. Place a 9 mm diameter silicone gasket on top of the PDMS microholes and spot the cell culture onto the holes (Figure 7cii).
53. Place the coverslip on a flat-bottomed centrifuge rotor and cover it with a hard plastic bottle cap taped down to the plate adapter. This is to prevent significant amounts of liquid evaporation during centrifugation. Use an appropriate weight balance.
54. Centrifuge the cells into the holes for 4 min at 3,220 rcf (Figure 7ciii).
55. Remove the silicone gasket. Rinse off excess cells from the PDMS surface using media by holding the coverslip upside down over a waste container and gently pipetting 1-2 mL media over the surface (Figure 7civ). The liquid on the PDMS surface should appear clear. If it remains turbid, rinse

with more media. **CRITICAL STEP:** If the washing step is not thorough enough, the pad will be covered in horizontal cells covering up the vertically immobilized cells (Figure 6b). If the pad is washed too aggressively, the vertically immobilized cells will be flushed out of the microholes. The washing step is also important to maintain hydration of the pad after centrifugation. **?TROUBLESHOOTING.**

56. Dab with a tissue to dry off the edges of the PDMS. Be careful not to dry off the region near the holes themselves. **CRITICAL STEP:** Ensure there is only a thin layer of liquid remaining on top of the holes. Too much liquid can result in a poorly-sealed chamber as liquid spreads under the double-sided tape, but too little liquid runs the risk of dehydrating the cells.
57. Seal the chamber together by peeling off the plastic covering of the double-sided chamber on the top of the flow chamber (Figure 7d) and pressing the top of the fluidic chamber to the µVerCINI coverslip, ensuring that the groove in the tape is over the microholes (Figure 7d). Seal the chamber fully by pressing around the edges of the tape.

**B.3 Imaging with µVerCINI. TIMING 10 min – 12 hr**

**CRITICAL:** If doing live-cell imaging, Steps 58-68 should be done with a microscope that is surrounded by an incubation box pre-heated to the cell growth temperature. Failure to do so can result in temperature shock to the cells, compromising results.

58. Transport the slide to the microscope in a pre-warmed empty pipette tip box to reduce temperature fluctuations in the sample.
59. Make sure the high working-distance objective is inserted, and use the appropriate immersion oil.
60. Position the µVerCINI device above the objective. Place reservoirs of media inside the microscope incubation box, and place the inlet tubing into one of them. Connect the needle of the outlet tubing to a 20 mL syringe. Attach the syringe to the syringe pump.
61. Fill the chamber with media using the syringe pump operating in Withdraw mode for using the following settings: diameter = 6”, flow rate = 10 mL/s. Ensure media has flowed into the chamber (~10 s). By operating in Withdraw mode, any failure to seal the chamber will result in the syringe pump pulling air rather than causing messy leaks in the microscope body. **?TROUBLESHOOTING.**
62. Change flow rate to something lower (e.g. 1.1 mL/s) for a slower, steady flow.
63. Using brightfield illumination, identify an area of the µVerCINI slide with a high loading efficiency and a low number of horizontal cells on top of the PDMS. **?TROUBLESHOOTING.**
64. Using fluorescence microscopy, take snapshots to scan the Z-plane to find the structure you wish to image.
65. Use an autofocus method of choice to maintain focus lock. We use an image-based system using a separate infrared brightfield pathway with a custom Micro-Manager plugin[12], although other methods may be applied.
66. Record a short brightfield time lapse as a control. This allows later identification of wobbling cells which can affect apparent protein dynamics. We recommend recording ~20 frames over ~1 s.
67. Record fluorescence with desired settings.
68. To change fluids during imaging, move the inlet tubing from one reservoir to another. **?TROUBLESHOOTING.**

*End of optional protocol steps, remaining protocol steps are common for both VerCINI and µVerCINI.*

**Image processing and analysis (Common to both VerCINI and µVerCINI). TIMING 30 min – 2 hr**

69. Select cells that are suitable for subsequent analysis by inspecting raw TIF files in Fiji or ImageJ.
    a. If a bright-field video was saved, exclude poorly trapped cells (these will appear to wobble in the holes due to diffusion). If the sample has been characterized previously, poorly trapped cells can be removed using the fluorescence video.

b. If a fluorescence Z-stack was saved, exclude cells where signal is not at the correct Z-plane.

70. Produce videos of cropped, denoised rings using the VerciniAnalysisJ Action Bar.
    a. Draw a 60x60 pixel ROI around each usable cell and record the position in the ImageJ ROI Manager. Click 'Save ROIs' to create a compressed folder containing positions of identified cells in the same directory as the TIF file.
    b. Click 'Batch denoise+register+crop' and select the directory containing the TIF and zip files. The output will be a denoised and registered TIF file of the full FoV and a folder called 'Indiv_rings' containing each cell cropped to the selected ROI. *Note:* the denoising step may take some time (>0.5 hrs) for large datasets.
71. Subtract the cytoplasmic backgrounds and produce circumferential kymographs using the testVerciniAnalysis script in MATLAB.
    a. Copy and paste the file testVerciniAnalysis.m from the directory ring-fitting2/testing into the Indiv_rings folder.
    b. Open testVerciniAnalysis.m in MATLAB and change any options as required, especially the *fname* variable defining the files you want to analyse. More information about options can be found in the documentation in the GitHub repository. Detailed documentation of all the optional arguments to the VerCINI software may be accessed by typing *'doc verciniAnalysis*' *or 'doc manualVerciniAnalysis'* in MATLAB*.* As the VerCINI circle-fitting method is performed on a per-frame basis, the analysis method works equally well on septa that constrict noticeably over the data acquisition period. In this case, analysis of constriction rate can also be performed as the cell radius for each frame is returned as a parameter of the analysis.
    c. Run the testVerciniAnalysis script. A new directory Indiv_rings/analysed is created containing the kymograph (with and without background subtraction), and the background subtracted VerCINI movie.

**Kymograph analysis. TIMING ~5 – 15 min**

72. Manually trace individual tracks in kymographs using VerciniAnalysisJ Action Bar in Fiji or ImageJ.
    a. Open the '_KymoRawWrap.tif' images to analyse.
    b. (Optional) Use 'Ridge Filter' in the Action Bar to highlight ridges in the image.
    c. For each image, use the straight line tool to trace over the kymograph lines and add the trace to the ROI manager.
    d. Click 'save ROIs' to create a compressed folder containing the traced lines in the same directory as the TIF file.
73. Once all of the kymographs have been traced, click 'Batch kymotrace statistics'.
    a. Define the camera pixel size and the frame interval of the images, then select the folder containing the TIF files and compressed ROI files. The results are output in a new ImageJ window and can be saved as a .csv file.

# TROUBLESHOOTING

| Step | Problem | Possible reason | Solution |
|---|---|---|---|
| 2 | The output from BEAMER is a row/ column of squares rather than a full array | The loops in series performing the translations are only keeping the final loop iteration | Change loop options to merge results of all iterations and repeat |
| 4 | The wafer is not uniformly covered with resist | Bubbles in the resist streaked across the wafer | Remove the resist layer by washing the wafer with acetone and repeat the spin-coating, careful to remove bubbles |

| | | | |
|---|---|---|---|
| 7 | There is still resist in unpatterned regions | The wafer was not developed long enough | Develop the wafer for another ~30 s in MF-321, soak in water, and dry |
| | All resist was dissolved after development | The wafer was not baked after the pattern was written | Repeat the resist coating, writing, and development (Steps 4-7) |
| 17 | The agarose pad is too thick or uneven | The agarose pad solidified too quickly as the microscope slide was pressed down on the wafer | Discard slide. Repeat Steps 13-17. Perform Step 17 on top of a hotplate set to 50°C. The higher temperature will give more time for the agarose to solidify while pressing down |
| 20 | The agarose pad stuck to the wafer after removing the slide | | Carefully peel the pad off the wafer and set it inside the Gene Frame with holes facing up |
| 22 | Cell culture is a dried smear on the pad | Cell culture dried out during centrifugation | Discard pad. Repeat Steps 13-22 with fresh pad, using a silicone gasket to hold the culture in place and a plastic cover to prevent evaporation |
| 29 | There are too many horizontal cells on the pad | Cells were not washed off sufficiently after loading | Discard slide. Repeat Steps 13-29, using extra media to wash off unloaded cells |
| | There are too few cells loaded into holes | Cells were washed off too aggressively after loading | Discard slide. Repeat Steps 13-29, being extra gentle with rinsing off unloaded cells |
| | | Cell culture was not concentrated enough | Discard slide. Repeat Steps 13-29, taking care to concentrate cell culture ~100× before spotting on pad |
| | | Hole widths are too small for cells | Search for a region of the pad with a larger hole size |
| | Most cells are wobbling in the holes | Hole widths are too large for cells | Search for a region of the pad with a smaller hole size |
| 39 | PDMS will not peel off the silicon wafer | The desiccator lost vaccum during the silanisation step, no passivation occurred | Try to carefully remove the PDMS and repeat the silanisation (Step 11) |
| | The coverslip breaks when peeling it off of wafer | Elastomer base : curing agent ratio was too high | Try to carefully remove the coverslip and repeat Steps 34-39 with lower ratio |
| | PDMS comes off silicon wafer easily, but will not come off back of coverslip | Elastomer base : curing agent ratio was too low | Discard the PDMS-covered coverslip and repeat Steps 34-39 with higher ratio |
| 48 | The needle punctures the tubing | The needle is being pushed while the tip is catching the inside wall of the tubing | Cut off the punctured segment of tubing. Repeat while bending the tubing away from the needle tip to avoid it catching the inside wall |

| | | | |
|---|---|---|---|
| 55 | Cell culture is a dried smear on the PDMS | Cell culture dried out during centrifugation | Discard coverslip. Repeat Steps 34-39, then Steps 49-55, careful to use a silicone gasket to hold the culture in place and a plastic lid to prevent evaporation |
| 61 | The chamber does not fill with media | The chamber is not sealed properly due to liquid under the tape | Discard the device. Repeat Steps 34-61 with a fresh device and, taking care to dry the PDMS outside the hole pattern in Step 56 prior to sealing with tape |
| | | The cut pipette tips are pressed against the PDMS and obstructing flow | Discard the device. Repeat Steps 34-61, careful to cut a few millimetres from the ends of pipette tips before inserting into drilled holes (Step 44) |
| 63 | There are too many horizontal cells on the PDMS | Cells were not washed off sufficiently after loading | Flush media through with a high flow rate for ~10 s to dislodge horizontal cells. Otherwise, discard the device and repeat Steps 34-63 |
| | The holes are filled with air bubbles rather than cells | The PDMS is too hydrophobic | Discard the device. Repeat Steps 34-63, careful to treat the PDMS-coated coverslip with plasma (Step 49) before loading cells |
| | There are too few cells loaded into holes | Cells were washed off too aggressively after loading | Discard device. Repeat Steps 34-63, being extra gentle with rinsing off unloaded cells |
| | | Cell culture was not concentrated enough | Discard device. Repeat Steps 34-63, taking care to concentrate cell culture ~100× before spotting on PDMS |
| | | Hole widths are too small for cells | Search for a region of the PDMS with a larger hole size |
| | Most cells are wobbling in the holes | Hole widths are too large for cells | Search for a region of the PDMS with a smaller hole size |
| 68 | Air is being pulled over tops of cells rather than liquid media | The reservoir of media is empty | Stop imaging. Discard device. Repeat Steps 34-68 using larger reservoir of media and/or lower flow rate |
| | | The inlet tubing is not in the media reservoir | Stop imaging. Discard device. Repeat Steps 34-68, careful that inlet tubing is resting at bottom of reservoir during imaging |

## TIMING

Steps 1-3, design of an array-of-squares pattern: 30 min – 2 hr, depending on speed of user

Steps 4-10, fabrication of a silicon micropillar wafer: ~3 hr

Steps 11-12, passivation and dicing of the silicon micropillar wafer: ~12 hr

*Silicon wafer fabrication total (Steps 1-12): ~16 hr*

Steps 13-17, preparation of VerCINI pads: ~20 – 40 min

Steps 18-26, loading cells into VerCINI pads: ~10 – 20 min

Steps 27-33, imaging with VerCINI: 10 min – 12 hr

*VerCINI total (Steps 13-33): 40 min – 12 hr*

Steps 34-48, preparation of μVerCINI device: ~2 hr

Steps 49-57, loading cells into μVerCINI coverslip: ~10 – 20 min

Steps 58-68, imaging with μVerCINI: 10 min – 12 hr

*μVerCINI total (Steps 34-68): ~2 – 12 hr*

Steps 69-71, image processing and analysis: 30 min – 2 hr, depending on size of dataset

Steps 72-73, kymograph analysis: ~5 – 15 min

*Analysis total (Steps 69-73): ~30 min – 2 hr*

## ANTICIPATED RESULTS

We have provided a detailed protocol for imaging vertically-confined bacterial cells using both VerCINI and μVerCINI. Using these methods, structures and biomolecular dynamics along the short axes of bacterial cells can be observed with high resolution without any special requirements for fluorophores or imaging modalities. VerCINI methods can also be combined with a wide range of other imaging methods (e.g. SIM or STORM) to provide greater resolution than is possible with each method individually.

Examples of results that a researcher can expect to obtain from VerCINI can be seen in Figures 1 and 2. With VerCINI, the treadmilling dynamics of the bacterial division protein FtsZ can be imaged with higher sensitivity than any other approach to-date[12] (Figure 1). Beyond this, VerCINI has also been used to track single molecules of both elongasome and divisome proteins moving circumferentially around the cell for minutes (ref [16] and our unpublished results), and to image the constricting division septum using STORM (ref [17] and our unpublished results). VerCINI also makes it possible to image cell pole proteins like TlpA at high resolution and SNR (Figure 2), paving the way for super-resolution studies to reveal the spatial organisation of these regions with unprecedented detail.

If researchers choose to use μVerCINI to image cells during antibiotic perturbations, they can expect to obtain results similar to those shown in Figure 3. We have used μVerCINI to observe the rapid effect of the FtsZ-targeting antibiotic PC190723 on FtsZ treadmilling dynamics across all stages of cell division. However, μVerCINI is compatible with many other experimental designs that include imaging during continual fluid flow or fluid exchange. This can include chemostatic growth[33], live-to-fixed cell imaging[34], or DNA-PAINT[35].

## CONCLUSION

Light microscopy of bacteria provides a wealth of information about their organisation, but conventional imaging approaches are limited to viewing bacteria along their long axes only. VerCINI provides a complementary approach by orienting bacteria vertically and imaging along their short axes, substantially improving the imaging of many biologically important structures and dynamic processes in non-spherical bacteria that were previously difficult to observe. VerCINI has already found multiple applications in high resolution imaging of bacterial spatial organisation in hands of a small number of early-adopter labs[5,12,13,15–17]. We hope that the methods and protocols presented here will allow many other labs to use VerCINI to look at diverse questions in bacterial cell biology from a different angle.

## Authorship Contribution Statement

KDW, SM, and CJ performed the experiments. KDW, SM, SH, and CD wrote the paper.

## Acknowledgements

We would like to acknowledge Sergii Pud (TU Delft; now at Twente) for help with wafer design and nanofabrication, Siddharth Deshpande (TU Delft; now at Wageningen) for help with nanofabrication and soft lithography, Marc Zuiddam (TU Delft) for help with wafer etching, Henrik Strahl (Newcastle) for strains and helpful discussions, and Joachim Fritzsche (ConScience AB, Sweden) for helpful discussions. SH, KDW, CJ, SM acknowledge funding support by a Wellcome Trust & Royal Society Sir Henry Dale Fellowship [206670/Z/17/Z]. CD acknowledges funding support by from the ERC Advanced Grants 883684 and 669598, and the NanoFront and BaSyC programs. SM supported by a UK Biotechnology and Biological Sciences Research Council doctoral studentship.

## Competing Interests

The authors declare no competing interests.

## Data availability

Source data for all figures presented in the paper are available at figshare:

https://doi.org/10.25405/data.ncl.c.5652010.v1

## Code availability

Custom software is available on the Holden lab GitHub page or Zenodo:

https://github.com/HoldenLab/VerCINI_nanofab[36]
https://github.com/HoldenLab/DeepAutoFocus[37]
https://github.com/HoldenLab/VerciniAnalysisJ[38]
https://github.com/HoldenLab/ring-fitting2[29]

## References

1. Huang, B., Babcock, H. & Zhuang, X. Breaking the Diffraction Barrier: Super-Resolution Imaging of Cells. *Cell* **143**, 1047–1058 (2010).
2. Pasquina-Lemonche, L. *et al.* The architecture of the Gram-positive bacterial cell wall. *Nature* **582**, 294–297 (2020).
3. Garner, E. C. *et al.* Coupled, Circumferential Motions of the Cell Wall Synthesis Machinery and MreB Filaments in B. subtilis. *Science* **333**, 222–225 (2011).
4. Domínguez-Escobar, J. *et al.* Processive Movement of MreB-Associated Cell Wall Biosynthetic Complexes in Bacteria. *Science* **333**, 225–228 (2011).
5. Bisson-Filho, A. W. *et al.* Treadmilling by FtsZ filaments drives peptidoglycan synthesis and bacterial cell division. *Science* **355**, 739–743 (2017).
6. Yang, X. *et al.* GTPase activity–coupled treadmilling of the bacterial tubulin FtsZ organizes septal cell wall synthesis. *Science* **355**, 744–747 (2017).
7. Kirkpatrick, C. L. & Viollier, P. H. Poles Apart: Prokaryotic Polar Organelles and Their Spatial Regulation. *Cold Spring Harb. Perspect. Biol.* **3**, a006809–a006809 (2011).
8. Kuwada, N. J., Traxler, B. & Wiggins, P. A. Genome-scale quantitative characterization of bacterial protein localization dynamics throughout the cell cycle. *Mol. Microbiol.* **95**, 64–79 (2015).
9. Laloux, G. & Jacobs-Wagner, C. How do bacteria localize proteins to the cell pole? *J. Cell Sci.* jcs.138628 (2014) doi:10.1242/jcs.138628.
10. Surovtsev, I. V. & Jacobs-Wagner, C. Subcellular Organization: A Critical Feature of Bacterial Cell Replication. *Cell* **172**, 1271–1293 (2018).
11. Bowman, G. R., Lyuksyutova, A. I. & Shapiro, L. Bacterial polarity. *Curr. Opin. Cell Biol.* **23**, 71–77 (2011).
12. Whitley, K. D. *et al.* FtsZ treadmilling is essential for Z-ring condensation and septal constriction initiation in Bacillus subtilis cell division. *Nat. Commun.* **12**, (2021).
13. Perez, A. J. *et al.* Movement dynamics of divisome proteins and PBP2x:FtsW in cells of Streptococcus pneumoniae. *Proc. Natl. Acad. Sci.* **116**, 3211–3220 (2019).

14. Chai, Y., Norman, T., Kolter, R. & Losick, R. An epigenetic switch governing daughter cell separation in Bacillus subtilis. *Genes Dev.* **24**, 754–765 (2010).
15. Söderström, B., Chan, H., Shilling, P. J., Skoglund, U. & Daley, D. O. Spatial separation of FtsZ and FtsN during cell division. *Mol. Microbiol.* **107**, 387–401 (2018).
16. McCausland, J. W. *et al.* Treadmilling FtsZ polymers drive the directional movement of sPG-synthesis enzymes via a Brownian ratchet mechanism. *Nat. Commun.* **12**, 609 (2021).
17. Trouve, J. *et al.* Nanoscale dynamics of peptidoglycan assembly during the cell cycle of Streptococcus pneumoniae. *Curr. Biol.* S0960982221005765 (2021) doi:10.1016/j.cub.2021.04.041.
18. Bakshi, S., Choi, H. & Weisshaar, J. C. The spatial biology of transcription and translation in rapidly growing Escherichia coli. *Front. Microbiol.* **6**, 636 (2015).
19. Zhou, Z. *et al.* The contractile ring coordinates curvature-dependent septum assembly during fission yeast cytokinesis. *Mol. Biol. Cell* **26**, 78–90 (2015).
20. Thiyagarajan, S., Munteanu, E. L., Arasada, R., Pollard, T. D. & O'Shaughnessy, B. The fission yeast cytokinetic contractile ring regulates septum shape and closure. *J. Cell Sci.* jcs.166926 (2015) doi:10.1242/jcs.166926.
21. Wollrab, V., Thiagarajan, R., Wald, A., Kruse, K. & Riveline, D. Still and rotating myosin clusters determine cytokinetic ring constriction. *Nat. Commun.* **7**, 11860 (2016).
22. Strahl, H. *et al.* Transmembrane protein sorting driven by membrane curvature. *Nat. Commun.* **6**, (2015).
23. Briegel, A. *et al.* New Insights into Bacterial Chemoreceptor Array Structure and Assembly from Electron Cryotomography. *Biochemistry* **53**, 1575–1585 (2014).
24. Deshpande, S. & Dekker, C. On-chip microfluidic production of cell-sized liposomes. *Nat. Protoc.* **13**, 856–874 (2018).

25. de Jong, I. G., Beilharz, K., Kuipers, O. P. & Veening, J.-W. Live Cell Imaging of Bacillus subtilis and Streptococcus pneumoniae using Automated Time-lapse Microscopy. *J. Vis. Exp.* 3145 (2011) doi:10.3791/3145.
26. Ellefsen, K. L., Dynes, J. L. & Parker, I. Spinning-Spot Shadowless TIRF Microscopy. *PLOS ONE* **10**, e0136055 (2015).
27. McGorty, R., Kamiyama, D. & Huang, B. Active microscope stabilization in three dimensions using image correlation. *Opt. Nanoscopy* **2**, 3 (2013).
28. Schindelin, J. *et al.* Fiji: An open-source platform for biological-image analysis. *Nat. Methods* **9**, 676–682 (2012).
29. Seamusholden & Kdwhitl. *HoldenLab/ring-fitting2: v1.1.2.1*. (Zenodo, 2021). doi:10.5281/ZENODO.4570259.
30. Luisier, F., Vonesch, C., Blu, T. & Unser, M. Fast interscale wavelet denoising of Poisson-corrupted images. *Signal Process.* **90**, 415–427 (2010).
31. Thevenaz, P., Ruttimann, U. E. & Unser, M. A pyramid approach to subpixel registration based on intensity. *IEEE Trans. Image Process.* **7**, 27–41 (1998).
32. Jakobs, M. A., Dimitracopoulos, A. & Franze, K. KymoButler, a deep learning software for automated kymograph analysis. *eLife* **8**, e42288 (2019).
33. Wang, P. *et al.* Robust Growth of Escherichia coli. *Curr. Biol.* **20**, 1099–1103 (2010).
34. Tam, J. *et al.* A Microfluidic Platform for Correlative Live-Cell and Super-Resolution Microscopy. *PLoS ONE* **9**, e115512 (2014).
35. Almada, P. *et al.* Automating multimodal microscopy with NanoJ-Fluidics. *Nat. Commun.* **10**, 1223 (2019).
36. Whitley, Kevin. *VerCINI_nanofab*. (Zenodo, 2021). doi:10.5281/ZENODO.5548030.
37. Whitley, K. D. *et al. DeepAutoFocus*. (Zenodo, 2021). doi:10.5281/ZENODO.4573121.
38. Seamusholden. *HoldenLab/VerciniAnalysisJ: v1.1.1*. (Zenodo, 2021). doi:10.5281/ZENODO.4617277.

39. Bisson-Filho, A. W. *et al.* Erratum for the Report: “Treadmilling by FtsZ filaments drives peptidoglycan synthesis and bacterial cell division”. *Science* **367**, (2020).
40. Tinevez, J.-Y. *et al.* TrackMate: An open and extensible platform for single-particle tracking. *Methods* **115**, 80–90 (2017).

**Figures:**

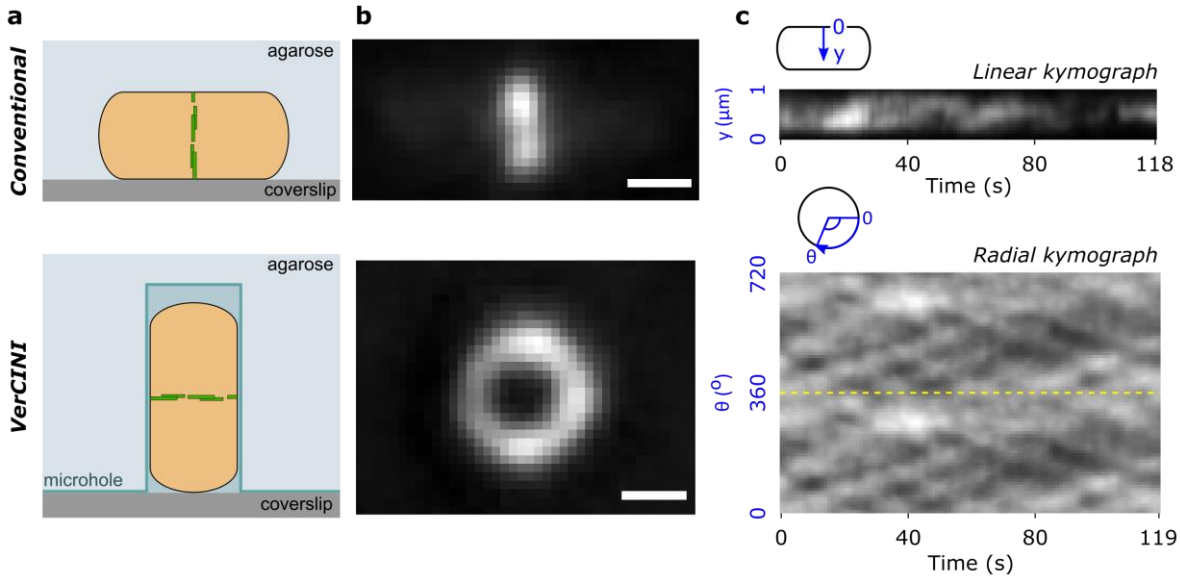


**Figure 1: Concept of VerCINI and comparison to conventional imaging of division protein dynamics.** (a) Schematics comparing conventional imaging and VerCINI to image division protein dynamics in rod-shaped cells. Division rings depicted as green dashed lines. *Top:* A cell lying horizontally under an agarose pad, with its division ring orthogonal to the microscope coverslip. *Bottom:* A cell confined vertically in an agarose microhole, with its division ring parallel to the microscope coverslip. (b) Representative images of *B. subtilis* cells expressing labelled FtsZ. *Top:* TIRF illumination of a cell expressing mNeonGreen-FtsZ ectopically from an inducible promoter (strain bWM4[39]). The bottom of the division ring appears as a line across mid-cell. *Bottom:* HiLO illumination of a cell expressing FtsZ-GFP as a sole copy of FtsZ from the native locus (strain SH130[12]). The full division ring appears as a circle. Scale bars: 500 nm. (c) Kymographs of FtsZ treadmilling dynamics from cells in (b). *Top:* Kymograph of mNeonGreen-FtsZ treadmilling dynamics from 0-1 µm across the short axis of the cell. Diagonal lines show directional motion across the short axis of the cell. *Bottom:* A kymograph of FtsZ-GFP treadmilling dynamics around the cell circumference. Two full revolutions around the cell (0-720°) are plotted side-by-side to resolve filament trajectories that cross 0°/360°, separated by a yellow dotted line. Diagonal lines show directional motion around the full circumference of the cell. Raw data from Whitley, Jukes et al. (2021)[12].

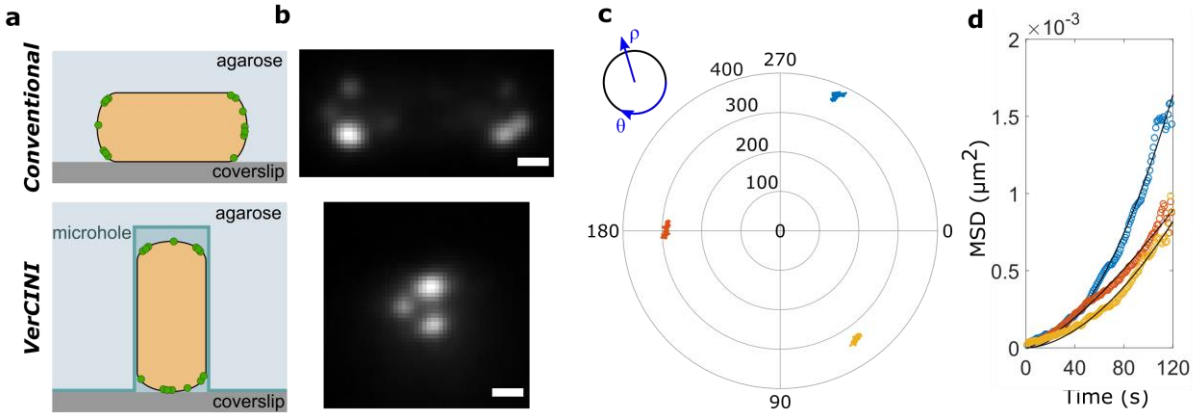


**Figure 2: Concept of VerCINI and demonstration to conventional imaging of polar protein dynamics.** (a) Schematics comparing conventional imaging and VerCINI to image polar proteins in rod-shaped cells. Polar proteins are depicted as green circles. *Top:* A cell lying horizontally under an agarose pad, with its poles orthogonal to the microscope coverslip. *Bottom:* A cell confined vertically in an agarose microhole, with its poles parallel to the microscope coverslip. (b) Representative images of *B. subtilis* cells expressing TlpA-mGFP ectopically from an inducible promoter (strain HS48[22]; Supplementary Methods). *Top:* Using conventional imaging with HiLO illumination the proteins appear as unresolved blobs at cell poles. *Bottom:* Using VerCINI with TIRF illumination, the proteins appear in several discrete clusters. Scale bars: 500 nm. (c) Polar plot showing the motion of TlpA-mGFP clusters from the VerCINI imaging in panel (b). Motion of clusters tracked using TrackMate[40]. (d) Mean squared displacements of clusters in (c) for different time intervals (circles; colours correspond to those in (c)) with fits to generalized diffusion equation $\langle r^2(t)\rangle = K_\alpha t^\alpha$ (black lines).

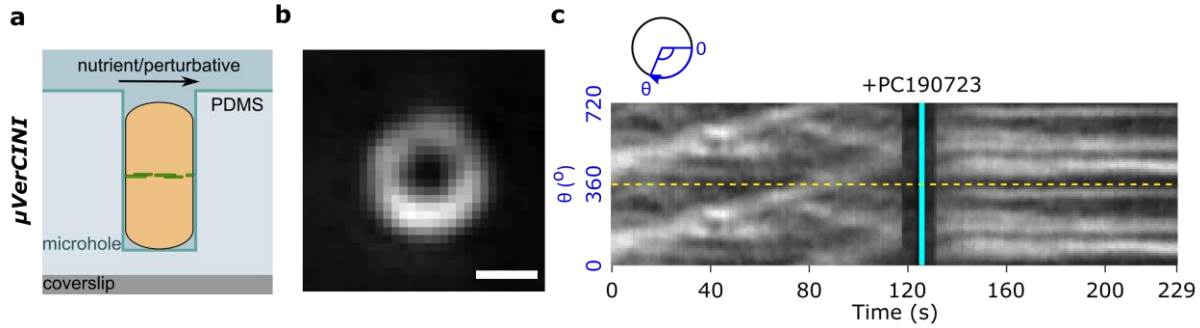


**Figure 3: Concept of μVerCINI and demonstration of imaging division protein dynamics during rapid antibiotic perturbation.** (a) Schematic depicting a cell confined vertically in an open-topped PDMS microhole inside a microfluidic chamber, with its division ring (green dashed lines) parallel to the microscope coverslip. (b) Representative image of a *B. subtilis* cell expressing FtsZ-GFP as a sole copy of FtsZ from the native locus (strain SH130[12]). The division ring appears as a circle. Scale bar: 500 nm. (c) Kymograph of FtsZ-GFP treadmilling dynamics from the cell in (b) around the cell circumference, during perturbation with the FtsZ-specific inhibitor PC190723 (cyan line). Two full revolutions around the cell (0-720°) are plotted side-by-side to resolve filament trajectories that cross 0°/360°, separated by a yellow dotted line. Diagonal lines pre-treatment show directional motion around the full circumference of the cell, while horizontal lines post-treatment show static clusters. Raw data from Whitley, Jukes et al. (2021)[12].

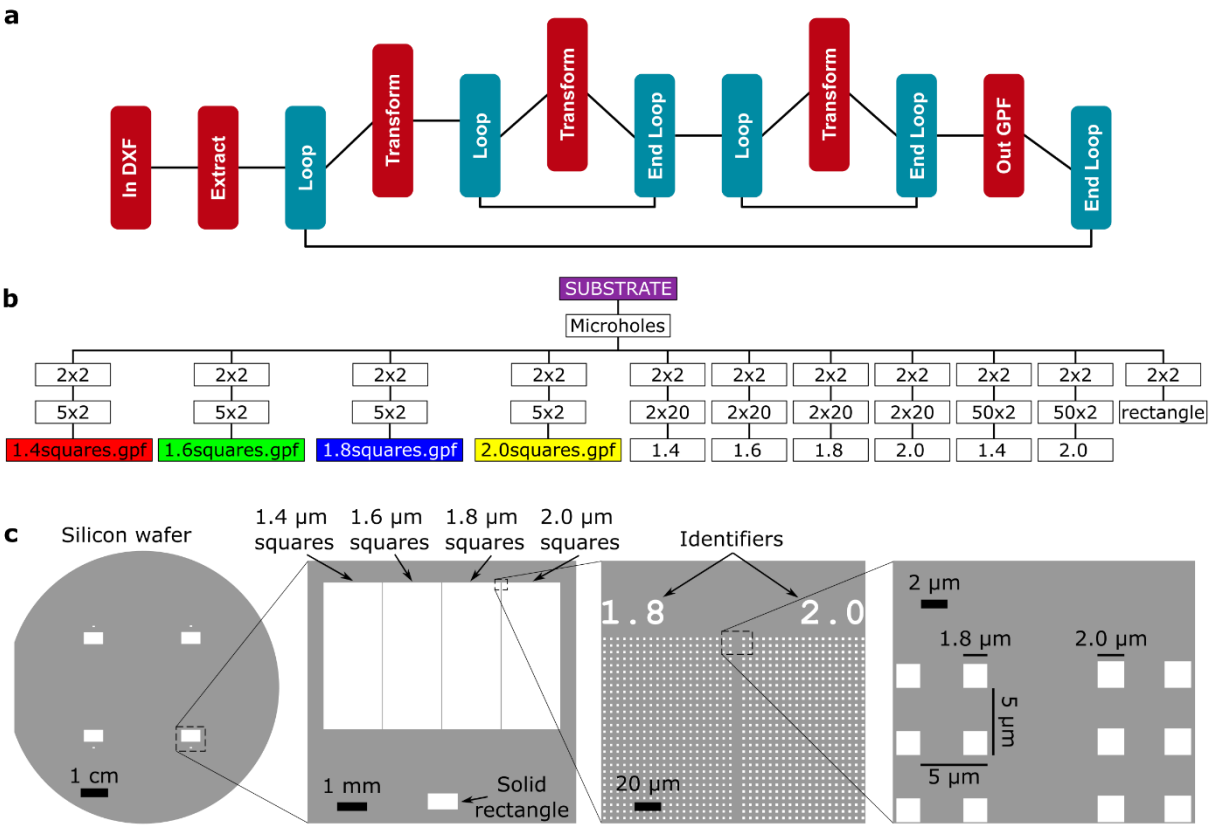


945 **Figure 4: Design of micropillar wafer.** (a) Algorithm of LayoutBEAMER used to produce arrays of
946 squares the size of the e-beam machine's main field. (b) Algorithm of Cjob used to produce full arrays
947 of squares of four different sizes in each quadrant of a wafer, along with identifiers and solid rectangle
948 for measuring height after etching. (c) Output of Cjob code and overall design of silicon wafer showing
949 arrays of squares of four different sizes in each quadrant of the wafer, along with identifiers and solid
950 rectangle.

951

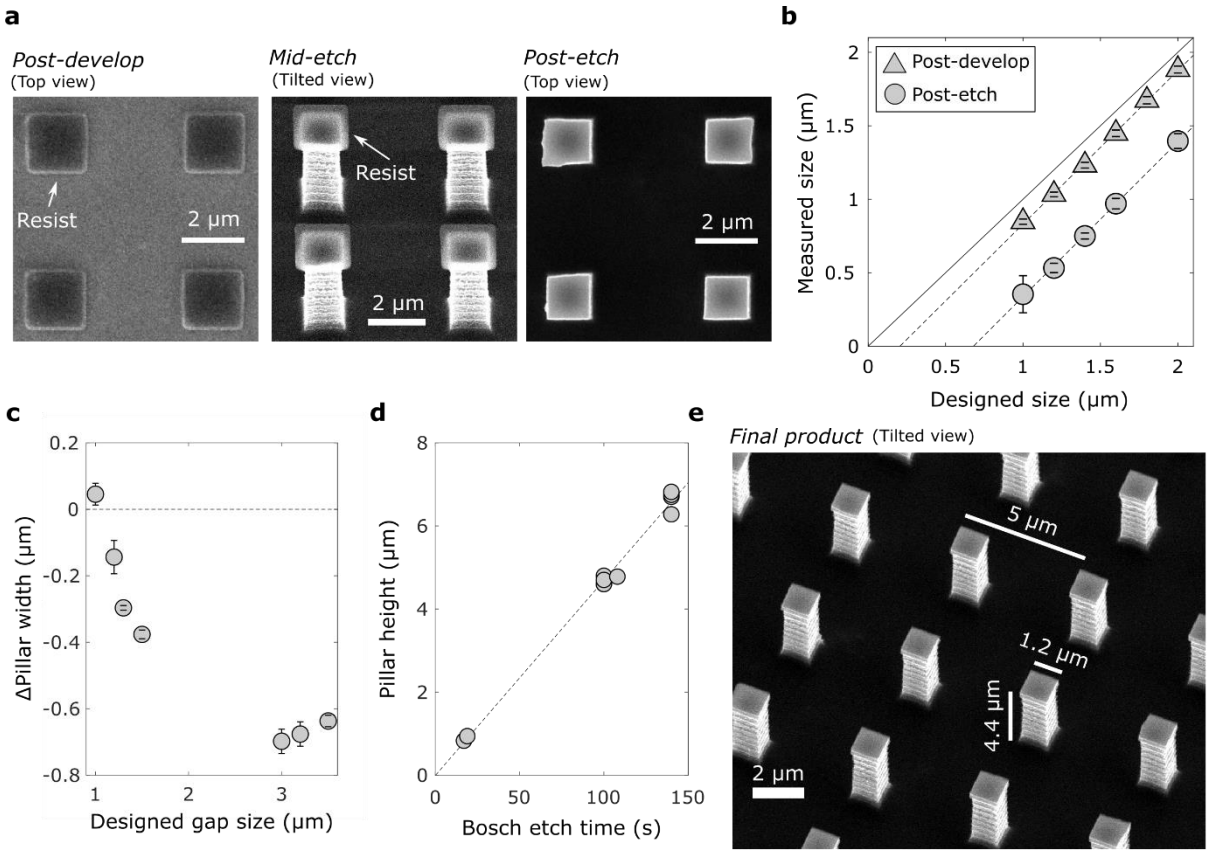


**Figure 5: Development and etching of micropillar wafer.** (a) SEM image of silicon wafer with squares with designed edge lengths of 2.0 μm during development and etching. *Left panel:* Patterned squares of e-beam resist remaining after development, seen from top down. *Middle panel:* Patterned squares after several cycles of Bosch etch, but before removing resist with oxygen plasma, seen from a tilted angle. Etching produces significant undercutting. *Right panel:* Patterned squares after etching and oxygen plasma to remove resist, seen from top down. Scale bars: 2 μm. (b) Comparison of designed square sizes to measured square sizes after development (triangles) and after 100 s of Bosch etch (circles). Solid line shows hypothetical 1:1 correlation. Dotted lines show linear fits to post-develop and post-etch data. Error bars are SD. (c) Change in widths of pillars after 140 s Bosch etch compared to designed size of gaps between pillars. Error bars are SD. (d) Effect of etch duration on final heights of micropillars. Each circle represents a separate wafer or wafer quarter. Wafers had different square sizes, but all had spacing of 5 μm. Dotted line: linear fit to data. (e) SEM image of a final silicon micropillar wafer with measured widths ~1.2 μm and spacing 5 μm (and hence gap of 3.8 μm between pillars). Heights were measured to be 4.4 μm from profilometer.

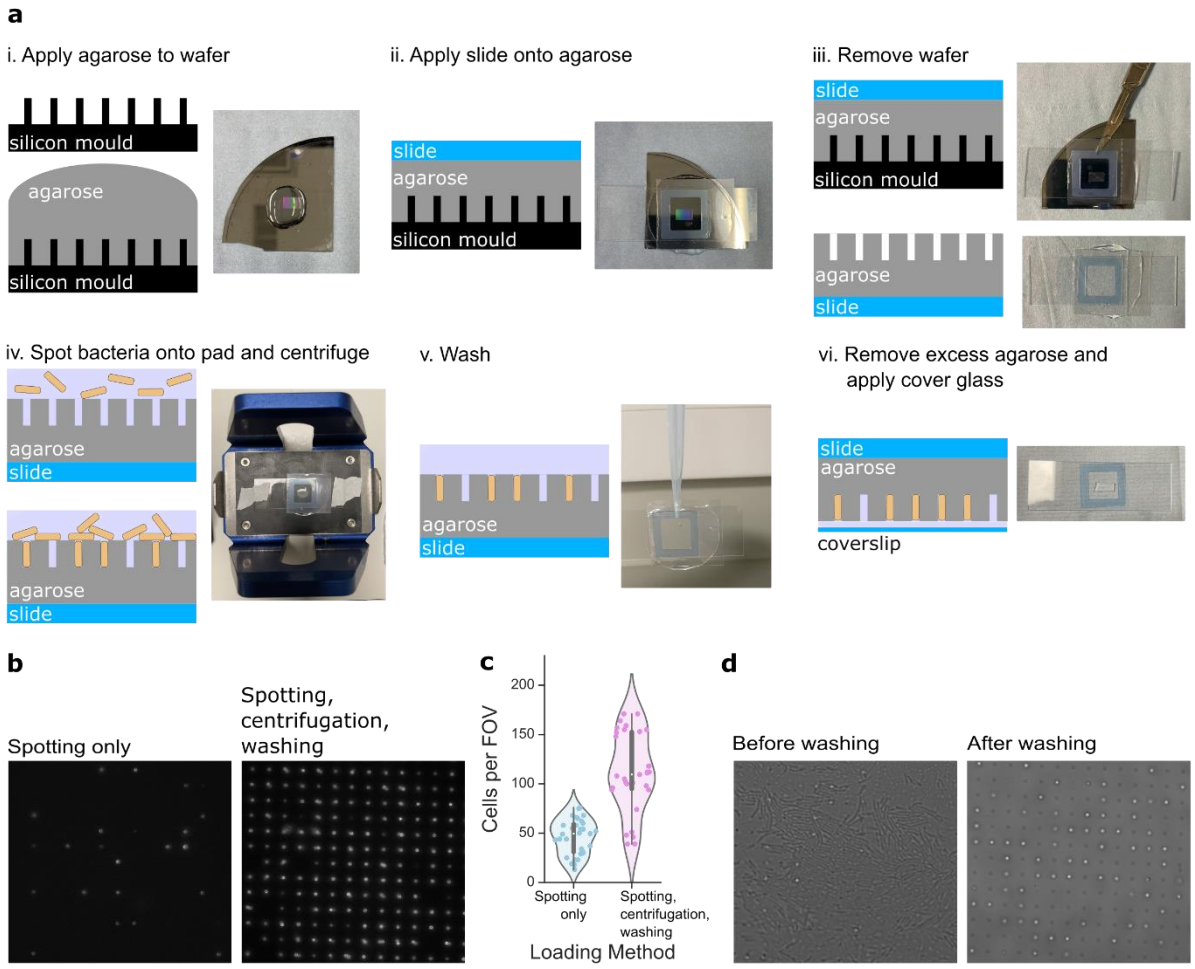


**Figure 6: Sample preparation for VerCINI.** (a) Sample preparation workflow. (i) Molten agarose is applied to the silicon micropillar wafer. (ii) The cover slide is applied onto the agarose with Gene Frame down. (iii) The micropillar wafer is removed from the agarose slide. (iv) Concentrated bacteria are pipetted onto the imprinted agarose, and the slide is centrifuged to increase loading efficiency. (v) Excess horizontal cells are washed off the pad. (vi) Excess agarose is cut away from the pad, leaving only the microhole imprinted area and the cover glass is applied. (b) HILO VerCINI of *B. subtilis* cells expressing FtsZ-GFP (strain SH130[12]) loaded into microholes with or without centrifugation. *Left*: cells loaded only by spotting liquid culture onto the VerCINI pad and applying the coverslip. *Right*: cells loaded by spotting concentrated liquid culture, centrifuging, and washing off unloaded cells. (c) Violin plots comparing of loading efficiency between the two loading methods shown in (b). White circles, median; thick grey lines, interquartile range; thin grey lines, 1.5x interquartile range. (d) Brightfield images of SH130, before and after the washing step.

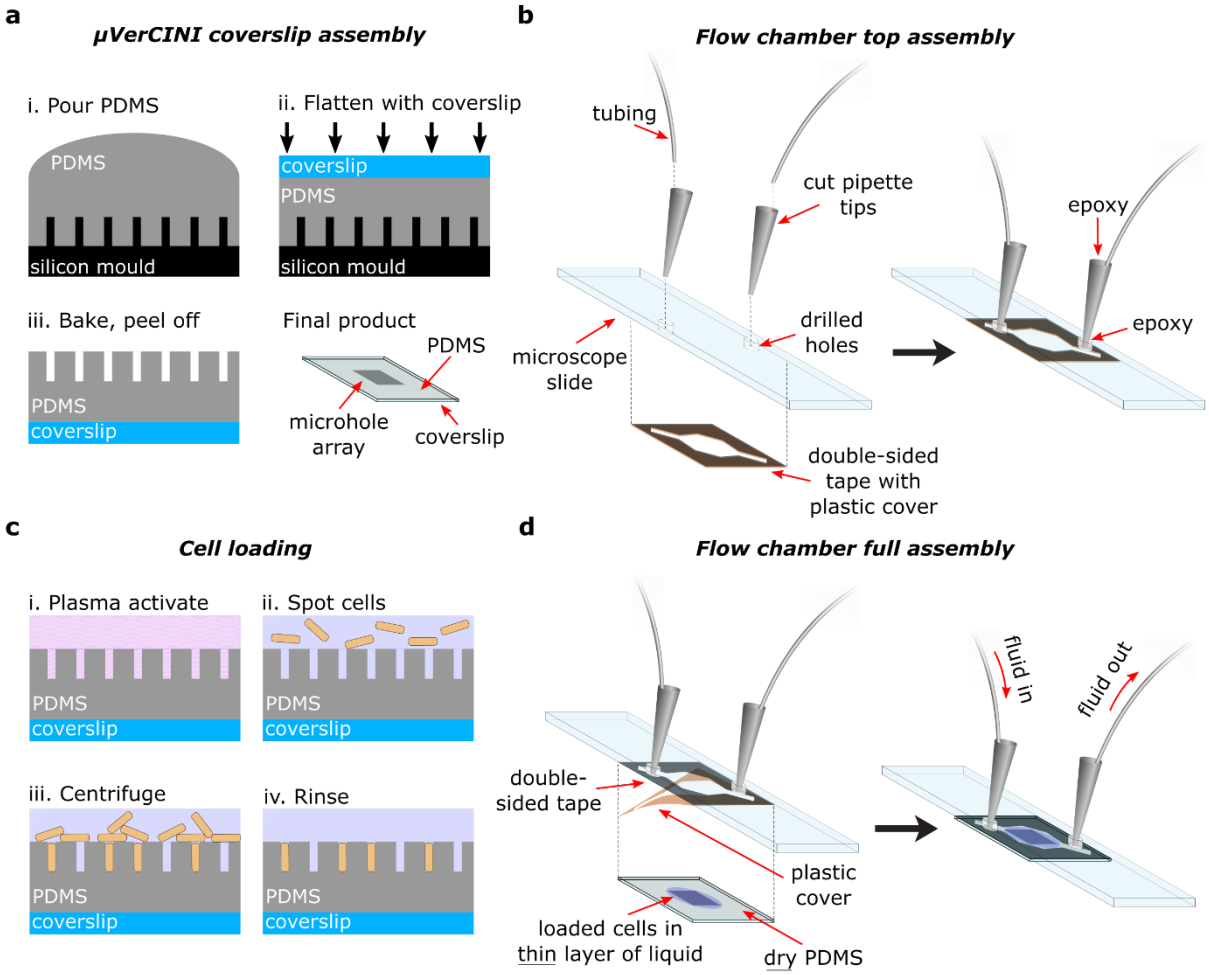


**Figure 7: Device assembly and cell loading for µVerCINI.** (a) Assembly of µVerCINI coverslip. (i) Degassed PDMS in a 10:1 elastomer base : curing agent ratio is poured onto silicon micropillars. (ii) A coverslip is pressed firmly down on top of the PDMS to form as thin a layer as possible. (iii) The PDMS is baked in an oven and peeled off to produce a coverslip with open-topped PDMS microholes. The final product can be stored for months to years. (b) Assembly of top of flow chamber. A microscope slide has holes drilled into it. Cut pipette tips are inserted into these holes and epoxied in place, and tubing is inserted into the cut pipette tips and epoxied in place. A piece of double-sided tape with plastic cover still attached has a groove cut into it and is adhered to the microscope slide. The final product can be stored for months to years. (c) Loading cells into open-topped microholes. (i) PDMS is rendered hydrophilic through treatment with air or oxygen plasma. (ii) Cell culture is concentrated and added on top of the microholes. (iii) The µVerCINI coverslip with concentrated cell cultures is centrifuged to load cells into holes. (iv) Cells not loaded into holes are rinsed off with fresh media. (d) Assembly of full flow chamber with loaded cells. PDMS µVerCINI coverslip is dried around the edges, and all but a thin layer of liquid is left above the loaded cells. The plastic cover of the double-sided tape is removed and the tape is adhered to the PDMS. The final product is a closed chamber through which fluid can be flowed.

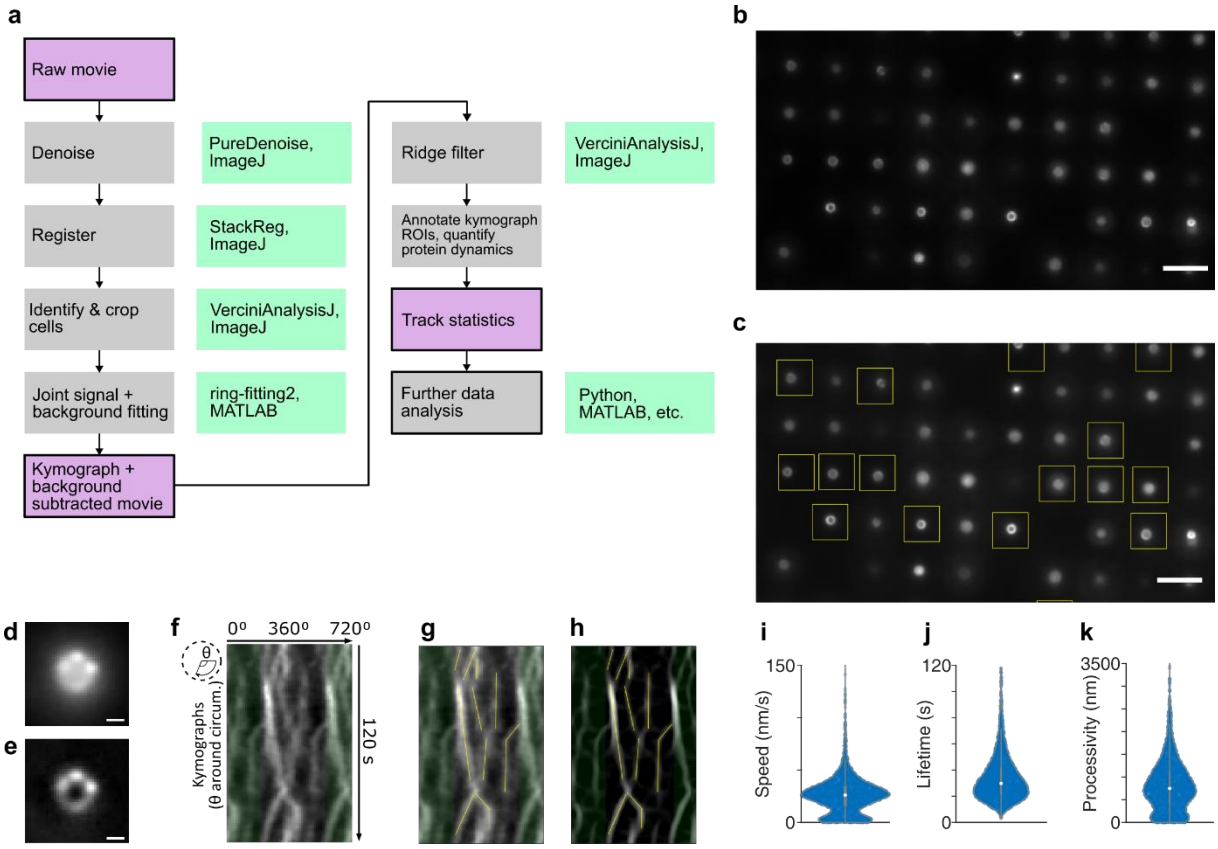


**Figure 8: Image processing and analysis for VerCINI and µVerCINI. (a)** VerCINI image processing workflow diagram. Purple box, data. Grey box, Image/ data processing step. Green box, software tool to perform image/ data processing step. **(b)** Exemplar VerCINI image of *B. subtilis* cells expressing FtsZ-GFP. Scale bar, 5 µm. **(c)** Regions of interest around in-focus cell septa/ circumference are manually identified and cropped for further analysis. Scale bar, 5 µm. **(d)** Exemplar denoised VerCINI image of a single cell. Scale bar, 0.5 µm. **(e)** Background subtracted image using joint model-based VerCINI fitting and background subtraction algorithm. **(f)** Kymograph around septum of background subtracted cell in *e*. **(g-h)** Annotated raw kymograph (g) and ridge-filtered kymograph (h). Line ROIs indicate manually detected and annotated filament trajectories. Green regions in f-h indicate repeated section of kymograph added to visualise filament trajectories crossing the boundary of the circular profile. **(i-k)** Exemplar violin plots of FtsZ-GFP filament dynamics measured by VerCINI. White circles, median; thick grey lines, interquartile range; thin grey lines, 1.5x interquartile range. Raw data in panels b-k from Whitley, Jukes et al. (2021)[12].

**Supplementary Information** contains methods specific for the data presented in Figure 2, including sample preparation, imaging, and data analysis.

**Supplementary Video 1: Suboptimal cell trapping visualized by brightfield microscopy.** *B. subtilis* PY79 cells improperly trapped in microhole arrays where microhole width (>1.1 μm) is too large to immobilize most cells. Lateral diffusive motion in the holes (wobbling) can be observed in ~50% of trapped cells. The video shows acceptable but not excellent cell loading efficiency. A few cells can be seen sitting on top of rather than within microholes, likely those that did not wash off during sample preparation. Video was recorded at 100 Hz and plays in real time. Scale bar: 10 μm.